

BEHAVIOR OF REINFORCED SAND SLOPE WITH A SOFT POCKET– EXPERIMENTAL AND NUMERICAL STUDY

Mostafa Abd Ellatif Elsawwaf¹, Waseim Rajab Azzam² and *Engy Mohamed Kassem³

Department of Structural Engineering, Tanta University, Egypt

*Corresponding Author, Received: 21 Feb. 2022, Revised: 08 March 2022, Accepted: 02 April 2022

Abstract: Soft pockets under the ground within the failure zone of the footing can ultimately pose substantial engineering problems including instability of the foundation, besides great super structural damage. Consequently, this paper aims to investigate the ultimate bearing capacity and the failure mechanism of a strip footing, loaded vertically on an un-reinforced and reinforced sand slope above a soft pocket. PLAXIS 3D Program was used to perform a series of finite element analyses on loaded strip footing, close to a sand slope with a soft pocket and the findings were investigated in detail, providing an analysis of the critical location of the soft pocket. The parameters affecting are the depth of the soft pocket below the strip footing, the setback distance between the slope crest and the footing, the relative density, and the number of reinforcement layers below the footing, which were all investigated. As indicated through the tests' findings, a soft pocket existing under the footing has a great impact on the stress and settlement of the footing. Moreover, the reinforcement layers included in the sand were the reason for not only a significant increase in the stability of the sandy slope but also for minimizing the settlement. Furthermore, the properties of the location of the footing relative to the slope crest and the depth of the soft pocket below the footing are the factors the efficiency of sand-geogrid depends on. Variations of the stress settlement with different parameters are provided and discussed based on the outcomes of the tests.

Keywords: Sand Slope Crest, Strip Footing, Soft Pocket, PLAXIS 3D, Geogrid Layers.

1. INTRODUCTION

The stability of the slope and the bearing capacity of a foundation placed near a slope's crest are regarded as fundamental factors in the performance of a structure built close to a slope. The foundation constructed on a sloping ground has one side exposed to the sloping surface and as a result, the foundation soil approaches limit state the plastic region of failure is very limited and it seriously affects the mechanical stability of the slope and thereby the bearing capacity of the foundation [1].

Furthermore, special attention is demanded in engineering practice to the presence of underground soft pockets or voids under rigid surface structures (e.g.; pavements, pipelines, and footings) and this is because soft pockets might influence the integrity of structures. If the soft pocket or void is located just below the footing at a shallow depth, the consequence can be very costly and dangerous. Mining, tunneling, water and gas networks, and aging conduits can all result in voids. With population growth and the resulting extension of urban sprawl to the areas of prior mining cavities as new cities in Egypt (Menia, Assuit, Sohage, Qena, et. al), geotechnical engineers are becoming increasingly concerned about foundation stability.

Using the finite element method, investigations were carried out into both the bearing capacity and failure mode of the footing above twin voids with changes in the voids' widths, diameters, embedded depths, eccentric distances, and the spacing between the voids [2]. Findings pointed out that bearing capacity declined as a result of the formation of twin voids below a surface footing, which depended on the system geometry.

The bearing capacity and failure mechanism of footings, placed on cohesive-frictional soils with voids, were studied and evaluated using discontinuity layout optimization [3]. The results indicate that the un-drained bearing capacity with voids is sensitive to soil weight and cohesion, as both the bearing capacity and stability issues exist. There is a direct relation between the mechanism of failure and various soil characteristics, the locations of single voids, and the horizontal distance between two voids. Yao et al. (2018) [4] investigated the bearing capacity of a strip footing on a rock mass with single or multiple continuous voids by using finite element limit analysis (FELA).

Makoto et al (2011) [5] reported model tests and analyses of the bearing capacity of strip footing on stiff ground with voids. Mohamed (2014) [6] studied the strip footing supported on a sand bed with an inside circular void by using PLAXIS and concluded that the bearing capacity of a strip footing decreases

with the decrease of the void depth and the increase of the diameter of the void.

Major analyses of previously conducted studies and papers have been found to focus on the behavior of loaded slope, with no consideration of the soft pocket within the soil. Moreover, the literature's main analysis gave more concern to studying the existence of such a soft pocket on the behavior of footing on level ground but neglected the sand slopes. However, it was noticeable that studying the behavior of loaded sand slopes with a soft pocket cannot be adequately investigated. Consequently, this paper aims to examine the ultimate bearing capacity and failure mechanism of a strip footing loaded vertically on an un-reinforced and reinforced sand slope with a soft pocket by using PLAXIS 3D Program to investigate the influences of such a soft pocket on the bearing capacity of a strip footing under the plane-strain condition. The derived findings are shown in various charts, and the critical failure mechanisms are described.

2. RESEARCH SIGNIFICANCE

This study discusses the problem of foundations, adjacent to slopes with a soft pocket, intending to measure the deformation behavior of the footing soil system reinforced by several geogrid layers, located near a sand slope with an embedded soft pocket. Such a problem is analyzed to safeguard foundations from collapse, and to control the settlement of footing and slope deformations, the research studies the ultimate bearing capacity and the failure mechanism of a strip footing vertically loaded on geogrid reinforced and un-reinforced sand slope above a soft pocket by using PLAXIS 3D Program.

3. FINITE-ELEMENT MODELING

The commercially available finite element program PLAXIS 3D version 2013 was used to model the strip footing on an un-reinforced and reinforced sand slope with a soft pocket. Fig. 1 shows the proposed model with the main geometric parameters included. A rigid strip footing with width (B) is placed on a sand slope of $2(V): 3(H)$. Where the setback distance between the slope crest and the strip footing was (b), the depth of the soft pocket below the footing was (Y), the width of the soft pocket was (w) and the length of the geogrid layers (L) was equal to $x+5B$, where (x) is a variable, which is related to the location depth of the geogrid layers [7]. Figure 2 shows a schematic sketch of the appropriate

mesh pattern considered in the present numerical analyses.

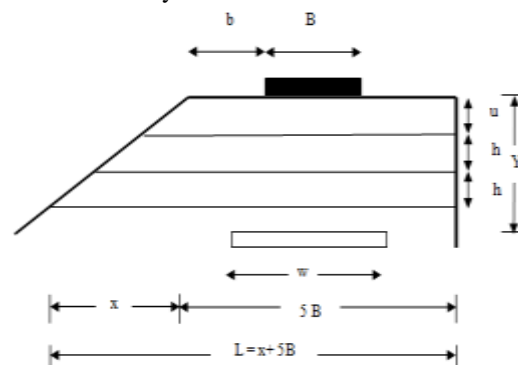


Fig. 1: Problem geometry.

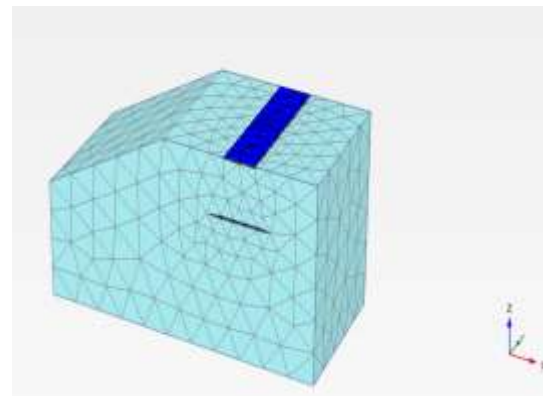


Fig. 2: Schematic mesh shape for numerical analyses in the present study.

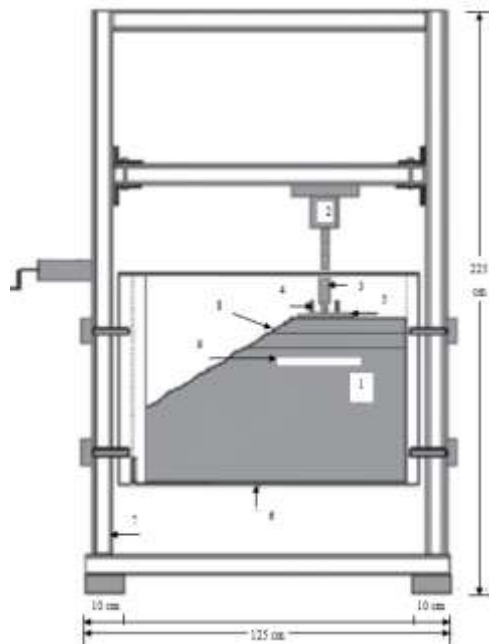
4. VERIFICATION OF NUMERICAL MODEL

To verify the capability of a numerical method, a comparison was made between the PLAXIS 3D software results with experimental study in the laboratory. Model experimental tests were carried out to study the bearing capacity of a strip footing supported on an un-reinforced and reinforced sand slope by geogrid with the existence of a soft pocket below the footing at the studied depth.

The testing tank is designed as a rigid steel box, 900 mm in length, 500 mm in height, and 400 mm in width (in the z-direction) as in Fig. 3. Also, the loading system was carried out according to [8,9,10]. In addition, the model testing tank satisfied the scale effects according to the previously mentioned studies.

The model strip footing was constructed of steel and included a hole in the top center to accommodate the bearing ball. Footing dimensions are 398 mm in length, 100 mm in width (B), and 20 mm in thickness. To maintain plane strain conditions throughout the confines of the test set-up, the strip footing was placed on the sand bed, with its length

equivalent to the width of the test tank [8,9,10].



- | | |
|--------------------|--------------------|
| 1. The sand soil, | 5. Strip footing, |
| 2. Hydraulic jack, | 6. Test tank, |
| 3. Load cell, | 7. The test frame, |
| 4. LVDTs | 8. Geogrid layer, |
| | 9. Styrofoam layer |

Fig. 3: Schematic diagram of the experimental apparatus (without scale).

5. MATERIAL AND METHODS USED FOR VERIFICATION EXAMPLE

5.1. Test Material

The tested sand used in this study is medium to coarse sand that has been cleaned, dried, and sorted by particle size. The particle size distribution was determined using the dry sieving method and the results are shown in Table 1.

The relative density achieved throughout the tests was measured by collecting samples in small cans of known volume placed at different locations in the tank [10,11,12,13]. The experimental verification provided a uniform relative density of approximately (D_r) 55% with a unit weight of 16.6 kN/m^3 . The internal friction angle of the sand and Young's modulus E were determined from a direct shear test using specimens prepared by dry tamping at the same relative density to be 37° and Young's modulus was $35000 \text{ (kN/m}^2)$.

Table 1. Properties of Sand Soil:

Property	Value
D_{10} (mm)	0.20

D_{60} (mm)	0.52
Uniformity coefficient, C_u	2.6
Coefficient of curvature, C_c	1.05
Specific gravity (kN/m^3)	2.63
Maximum dry unit weight (kN/m^3)	18.9
Minimum dry unit weight (kN/m^3)	14.4
Maximum void ratio	0.51
Minimum void ratio	0.39
Classification (USCS)	SP

5.2. Model of a Soft Pocket (S. P.)

Since Styrofoam is made up of 98% air, which makes it light and buoyant, a Styrofoam layer was used as a soft pocket in this study. Styrofoam was placed beneath the center of the footing, taking into consideration that both the Styrofoam and the footing are parallel [10,14]. The dimensions of Styrofoam were 400 mm in length (equivalent to the width of the tank as a strip layer below the strip footing), 200 mm in width (w) which is equal to $2B$, and 20 mm in thickness (the same thickness of the strip footing) in all the tests. As seen in Fig. 4, Styrofoam is a type of polystyrene foam that is typically white. The Elasticity modulus (E) KN/m^2 , the density of Styrofoam (kN/m^3), and Compressive strength (psi) were equal to 0.1200, 0.063, and 30, respectively according to the manufacturer.



Fig. 4: The model of an S.P. (Styrofoam layer).

5.3. Geogrid Reinforcement

Tensar TriAx Geogrid Layer was used as reinforcing material for this analysis as in Fig. 5. Typical physical and technical properties of the grids were obtained from a manufacturer's datasheet given in Table 2.



Fig. 5: Tensar TriAx Geogrid layer.

Table 2: The Properties of the Geogrid:

Description	Value
Type of polymer	100% polypropylene
Radial Secant Stiffness at 0.5% strain (kN/m)	275
Radial Secant Stiffness at 2.0% strain (kN/m)	205
Radial Secant Stiffness Ratio	0.75
Junction Efficiency %	100
Hexagon Pitch (mm.)	66
Weight (kg/m ²)	0.180

5.4. The Loading System and Experimental Setup

In the lab, a total of 16 tests were performed. The response of the model footing supported on un-reinforced level ground was initially determined (three tests with a soft pocket in different depths below the footing (Y/B=1.0, 1.5, and 2.0) and one test without a soft pocket) for the chosen relative density medium state ($D_r=55\%$). Then, three tests were performed to study the effect of the different depths of the soft pocket below the footing on a sand slope of 2(V): 3(H) at b/B=1.0, Y/B=1.0, 1.5, and 2.0, and one tests without a soft pocket. In addition, study the effect of the reinforcement system on improving the behavior of the footing at N=1 for both level ground and sand slope with and without the soft pocket.

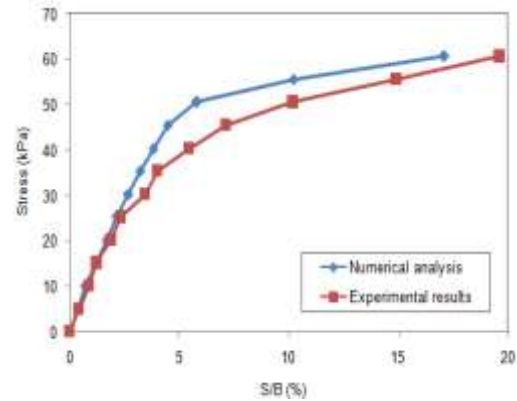
By using the findings obtained through the experimental test program of this study, the numerical model got its validation. As shown in Figs. 6 (a and b) which compare the stress-settlement curve for the experimental and theoretical analysis of a footing close to a slope (b/B=1.0) with and without a soft pocket. The experimental and current FE modeling have achieved good agreement. For further information, check the Bearing Capacity Ratio (BCR) values achieved from the FE analysis and the results obtained from the relevant experimental model tests as illustrated in Fig. 6 (c).

The effect of the geogrid layers on a sand slope with a soft pocket on the bearing capacity (B.C.) is estimated by Bearing Capacity Ratio (BCR) as:

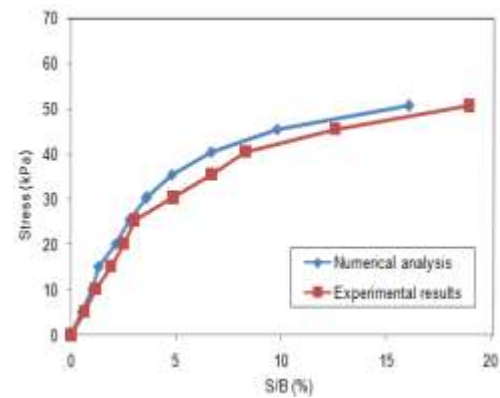
$$BCR = \frac{\text{Ultimate B. C. reinforced sand slope}}{\text{Ultimate B. C. un-reinforced sand slope}}$$

The figures illustrate that the FE results provide a reasonable fit with the experimental data and agree with the same trend. However,

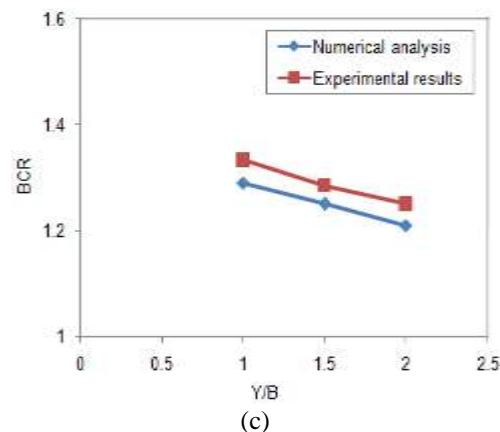
the degree of improvement in the bearing capacity of FE results is slightly higher than the experimentally predicted values by 5%. Consequently, the PLAXIS 3D (FEM) is capable of predicting the behavior of the problem under investigation.



(a)



(b)



(c)

Fig. 6: Comparison of experimental versus numerical results : (a) Variations of stress with settlement ratio (S/B) for footing on an un-reinforced sand slope without an S.P. for $D_r=55\%$; (b) Variations of stress with S/B for footing on an un-reinforced sand slope with an S. P. at Y/B=1.5 for $D_r=55\%$. (c) Variations of BCR versus Y/B at N=1.0.

6. FINITE ELEMENT ANALYSIS

The behavior of soils was numerically simulated considering the Mohr-Coulomb failure criterion. Table 3 shows the material properties used in PLAXIS 3D Program. In the numerical study, a uniform relative density of approximately (D_r) equals 55% and 80% has been used. The footing was positioned on the sand bed with the length of the footing equivalent to the full width of the soil. The footing was assumed linear and isotropic material with steel Young's modulus of $E=2.8e7$ (kN/m²) and Poisson's ratio $\nu=0.2$. The footing is connected to the soil via interface elements $R_{int}=0.65$ according to the manual.

Table 3: The properties of the material used in PLAXIS 3D:

Parameter	Dense Sand (D.S) R.D=80%	Medium Dense Sand (M.D.S) R.D=55%
	Young's Modulus E (kN/m ²)	50000
Cohesion C (kN/m ²)	0.0	0.0
Soil unit weight (γ) (kN/m ³)	17.7	16.6
Poisson's ratio ν	0.25	0.25
Friction angle (ϕ)	40.2	37
Dilatancy angle (Ψ)	10.2	7

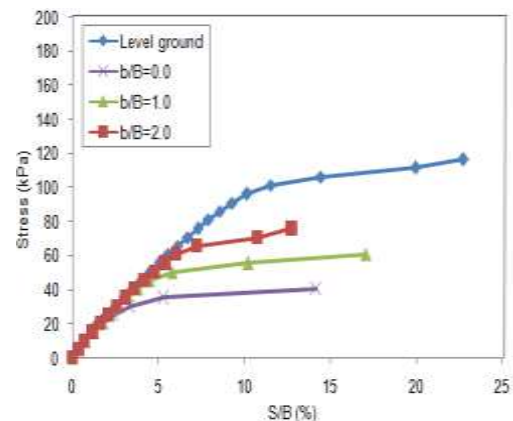
In total, 112 tests were performed in PLAXIS 3D. Firstly, the response of the model footing supported on the un-reinforced and reinforced level ground was evaluated (18 tests with a soft pocket in various depths below the footing and 8 tests without a soft pocket) for two chosen relative densities medium state ($D_r=55\%$) and dense state ($D_r=80\%$). Then, 13 series of tests (86 tests) were carried out to study the effect of the different parameters of a soft pocket on the footing behavior on a sand slope of 2(V): 3(H). Table 4 shows all of the test programs, including both constant and variable parameters.

7. THE NUMERICAL RESULTS AND DISCUSSION

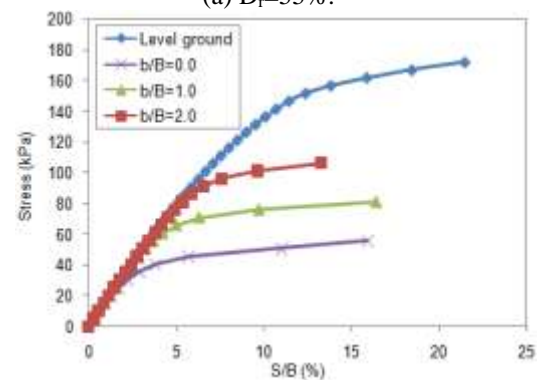
Using PLAXIS 3D Program, 112 runs in total were performed on a model of a strip footing on an un-reinforced and reinforced sand slope with an S.P.

The ultimate bearing capacity (ultimate B. C.) for the footing-soil systems is determined from the stress-settlement curves as the pronounced peaks, after which the footing collapses and the load decreases. In this study, there is no peak failure exhibited so, the ultimate B. C. was determined by choosing the tangent intersection method [1,6,10,15].

In Fig. 7 the findings show that the ultimate B. C. increases with increasing the setback distance between the footing and the slope crest. When the footing is moved away from the slope crest ($b/B=0$) to the setback distance at $b/B=2.0$, there is a serious increase in ultimate B. C. an average value of 75% and 72% for different sand relative densities. Also, (S/B) noticeably increased by 175% and 125% at ultimate B. C. for different sand relative densities.



(a) $D_r=55\%$.



(b) $D_r=80\%$.

Fig. 7: Variations of stress with (S/B) for a footing on sand without an S.P. for level ground and sand slope at different setback distances for different sand relative density.

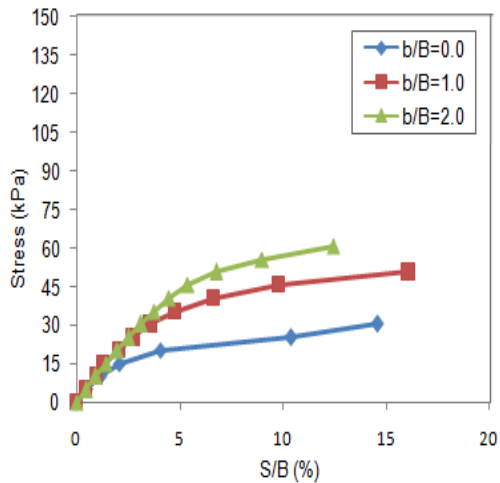
Table 4: Studied Program and Investigated Parameters adopted in the Numerical Program:

Series	Constant Parameters	Variable Parameters		
		$D_r=55\%$	$D_r=80\%$	
1	Un-reinforced level ground	No S. P., Y/B=1.0, 1.5, 2.0	No S. P., Y/B=1.0, 1.5, 2.0	
2	Un-reinforced sand slope, b/B=0	No S. P., Y/B=1.0, 1.5, 2.0	No S. P., Y/B=1.0, 1.5, 2.0	
3	Un-reinforced sand slope, b/B=1.0	No S. P., Y/B=1.0, 1.5, 2.0	No S. P., Y/B=1.0, 1.5, 2.0	
4	Un-reinforced sand slope, b/B=2.0	No S. P., Y/B=1.0, 1.5, 2.0	No S. P., Y/B=1.0, 1.5, 2.0	
5	Reinforced level ground, No S. P.	N=1, 2, 3	N=1, 2, 3	
6	Reinforced level ground, Y/B=1.0, N= 1	$D_r=55\%$ and $D_r=80\%$		
7	Reinforced level ground, Y/B=1.5	N=1, 2	N=1, 2	
8	Reinforced level ground, Y/B=2.0	N=1, 2, 3	N=1, 2, 3	
9	Reinforced sand slope, No S. P., $D_r=55\%$	b/B =0.0	b/B =1.0	b/B =2.0
		N=1, 2, 3	N=1, 2, 3	N=1, 2, 3
10	Reinforced sand slope, Y/B=1.0, N=1, $D_r=55\%$	b/B =0.0, 1.0, 2.0		
11	Reinforced sand slope, Y/B=1.5, $D_r=55\%$	N=1, 2	N=1, 2	N=1, 2
12	Reinforced sand slope, Y/B=2.0, $D_r=55\%$	N=1, 2, 3	N=1, 2, 3	N=1, 2, 3
13	Reinforced sand slope, No S. P., $D_r=80\%$	N=1, 2, 3	N=1, 2, 3	N=1, 2, 3
14	Reinforced sand slope, Y/B=1.0, N=1, $D_r=80\%$	b/B =0.0, 1.0, 2.0		
15	Reinforced sand slope, Y/B=1.5, $D_r=80\%$	N=1, 2	N=1, 2	N=1, 2
16	Reinforced sand slope, Y/B=2.0, $D_r=80\%$	N=1, 2, 3	N=1, 2, 3	N=1, 2, 3
17	Un-reinforced sand slope, b/B=1.0	Y/B=3.0, 4.0	Y/B=3.0, 4.0	
18	Reinforced sand slope, b/B=1.0, N=1	Y/B=3.0, 4.0	Y/B=3.0, 4.0	

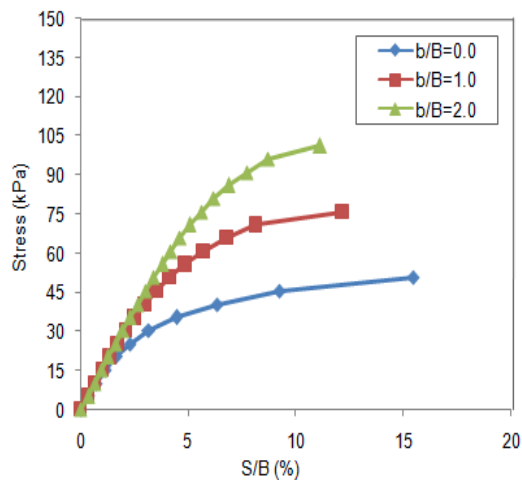
Note: See Fig. 1 for definition of the variable. (B)= 100 mm, (w) =2B which were always constant. In reinforced tests, (u/B) =0.50, (h/B)=0.5 were always constant [8,13], (N) is the number of the geogrid layers =1, 2 and 3 [16,17].

Fig. 8 illustrates the variations of stress with (S/B) for a footing on an un-reinforced sand slope with an S.P. at Y/B=1.5 for different sand relative densities. It can be observed that the ultimate B. C. got reduced by 69% and

67% at b/B=0.0 compared to b/B=2.0 for different sand relative densities. Despite that, (S/B) at the ultimate B. C. increased by 100% and 67% at b/B=2.0 compared to b/B=0.0 for different sand relative densities.



(a) $D_r=55\%$.

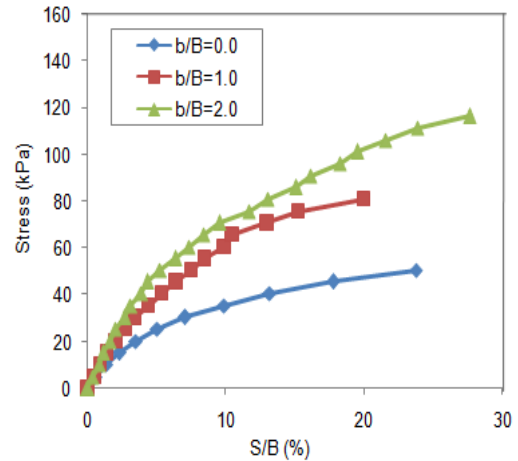


(b) $D_r=80\%$.

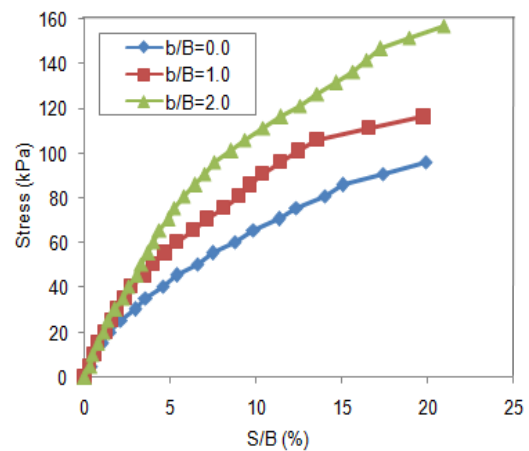
Fig. 8: Variations of stress with (S/B) for a footing on an un-reinforced sand slope with an S. P. at $Y/B = 1.5$ for a different sand relative density.

Fig. 9 shows the variations of stress with (S/B) for a footing reinforced sand slope with an S.P. at $Y/B = 1.5$ for a different sand relative density at $N=2.0$. It can be seen that the ultimate B. C. decreased by 68% and 36% at $b/B=0.0$ for reinforced sand slope compared to $b/B=2.0$ for a different sand relative density at $N=2$. Also, (S/B) at the ultimate B. C. decreased by 75% and 56% for a different sand relative density.

It is then concluded that when soil reinforcement is included, it acts more efficiently to reduce the footing settlement and hence improve the overall behavior of loaded footing on sand slopes above a soft pocket.



(a) $D_r=55\%$.



(b) $D_r=80\%$.

Fig. 9: Variations of stress with (S/B) for a footing on a reinforced sand slope with an S. P. at $Y/B = 1.5$ for a different sand relative density at $N=2.0$.

7.1. The Effect of the Number of the Geogrid Layers

The variation of BCR (Bearing Capacity Ratio) against the number of layers (N) at $Y/B=2.0$ and $b/B=1.0$ is shown in Fig. 10. It can be observed that the inclusion of soil reinforcement causes additional considerable improvements in the BCR of the footing which increases with an increase in the number of geogrid layers. When $N=1$ the BCR is 1.33 and when using $N=3$ it becomes 1.88 at $D_r=55\%$. However, this increase decreased to 1.154 and 1.69 at $N=1$ and 3, respectively at $D_r=80\%$.

This means that the BCR value increases slightly with decreasing sand relative density at any number of geogrid layers.

This can be attributed to the fact that in dense sand, the sand layer between the footing base and the soft pocket is more rigid than that for medium dense sand, which leads to the effect of surface footing load transferred to the soft pocket faster than that in medium sand [6,10].

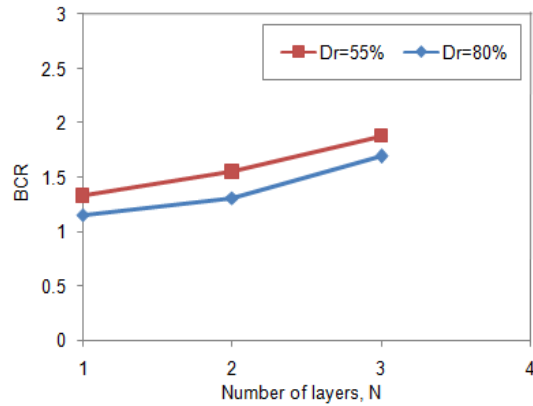
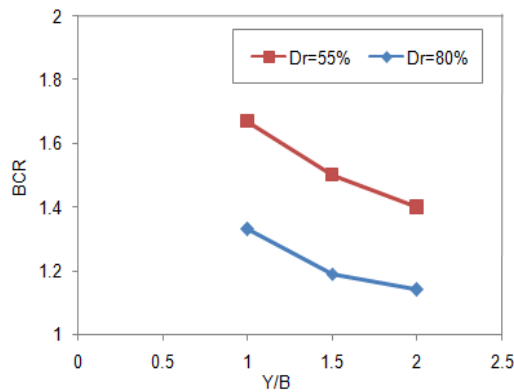


Fig. 10: Variations of BCR with several geogrid layers (N) at Y/B=2.0 and b/B=1.0 for a different sand relative density.

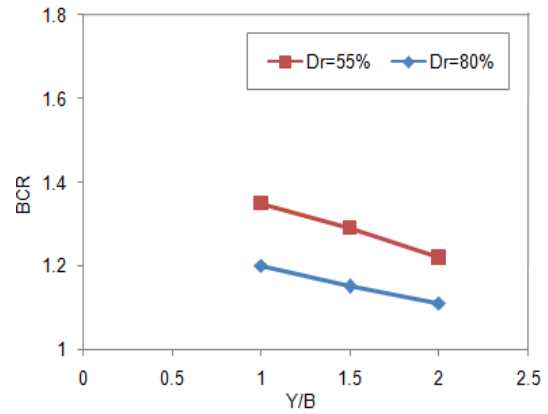
7.2. The Effect of the Depth of the Soft Pocket (S. P.) Below the Footing

Figure 11 demonstrates the variations of BCR with Y/B at N=1 for different sand relative densities at b/B=0.0, 1.0, and 2.0.

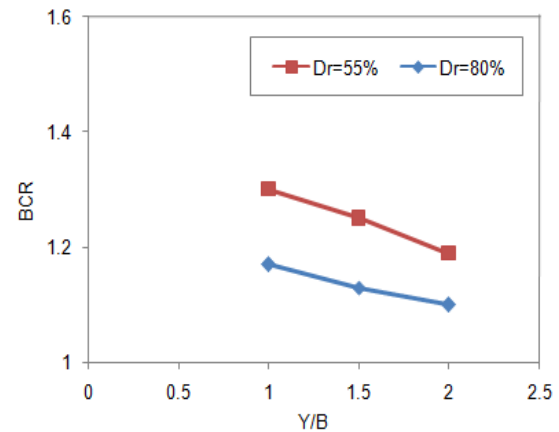
The ultimate B. C. of footing increases in response to an increase in the depth of a soft pocket below the footing where the stress-settlement ratios curve of footing approaches that corresponding to no S. P. condition. Based on that, it can be seen that the efficacy of the geogrid layer is found to be maximum when the depth of an S.P. below the footing is Y/B=1.0 where the BCR values decrease with increasing the depth of the S. P. (Y/B=2.0) [2,6,10].



(a) Variations of BCR for b/B=0.0.



(b) Variations of BCR for b/B=1.0.



(c) Variations of BCR for b/B=2.0.

Fig. 11: Variations of BCR with Y/B at N=1 for a different sand relative density.

Variations of BCR for various embedment depths of soft pockets (Y/B=1.0, 2.0 3.0, and 4.0) at N=1 and b/B=1.0 for a different sand relative density have been illustrated in Fig. 12. As discussed before, the ultimate B. C. of footing tends to increase by an increase in the depth of an S.P. It may be due to getting an S. P. away from the zone in which the failure mechanism is formed. Through extrapolation to the results in Fig.12, it can be realized that the impact of an S.P. on the B.C. of a shallow foundation approximately disappeared at about $(Y/B)_{cr} = 3$ [2]. It can also be noticed that by increasing the depth of the soft pocket further than that, there is an increase in BCR because there is a remarkable improvement in the sandy soil of medium density by using the geogrid, compared to the dense sand soil, where the ultimate B.C. was too low with the soft pocket, without the geogrid layer for the sand of medium density compared to dense sand soil.

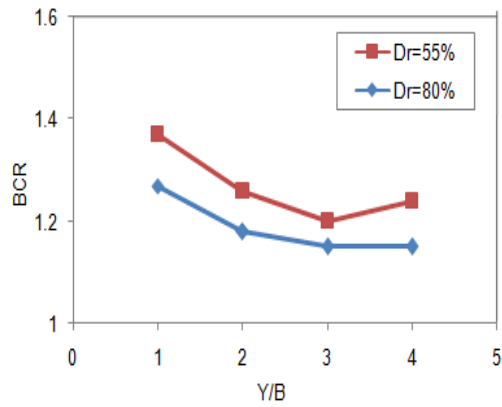


Fig. 12: Variations of BCR with Y/B at N=1 and b/B=1.0 for different sand relative densities.

7.3. The Effect of the Footing Location Relative to the Slope Crest

Fig. 13 shows the variations of BCR with b/B at Y/B=1.5 and N=2 for a different sand relative density. When the footing is positioned on the edge of the slope b/B=0.0, the efficacy of the geogrid layer is found to be at its greatest.

BCR decreases when the footing setback distance between the slope crest and the footing increases where, at b/B=2.0 and N=2, the efficiency of the geogrid layer is observed to be reduced beyond a footing [10,18].

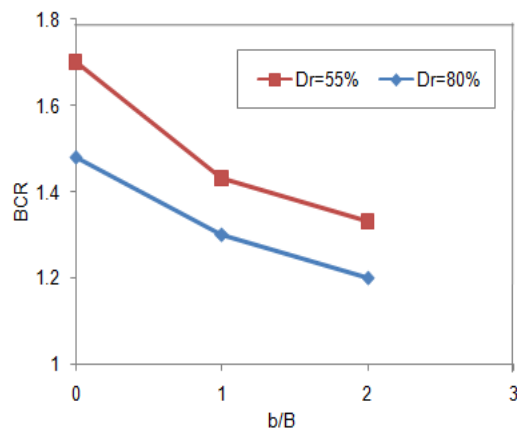


Fig. 13: Variations of BCR with b/B at Y/B=1.5 and N=2 for a different sand relative density.

8. THE FE BEHAVIOR OF THE PROTOTYPE

This investigation studies the ability to use the finite element program to solve a large-scale problem. Therefore, a large-scale model was carried out to examine the size and scaling effect. The validity and degree of improvement of ultimate B. C. for a strip footing adjacent to

an un-reinforced and reinforced sand slope above a soft pocket were investigated. The size of the large-scale model was (20x10x6)m to simulate the large-scale behavior. The properties of sand soil, soft pocket, and geogrid layers remained the same as in the original model scale studies.

The strip footing properties were taken as concrete footing [19]. Table 5 shows the properties of the concrete strip footing. The thickness of the strip footing and the height of the soft pocket was equal to 60 cm. Moreover, the width of the concrete strip footing was equal to 1.0 m in all the prototype models.

Table 5: Concrete properties used for strip footing:

Unit weight (γ) (kN/m ³)	Modulus of Elasticity (E) (kN/m ²)	Poisson's Ratio (ν)
25	2.2e7	0.15

A prototype problem was conducted to examine the size and scaling effect. Ten tests (two series) were carried out on model footing resting on an un-reinforced and reinforced sand slope above a soft pocket at different depths below the footing. Fig. 14 and 15 show the variations of BCR with the different depths of the soft pocket at Y/B=1.0, 1.5, 2.0, 3.0, and 4.0 with a large scale at b/B=1.0, N=1, and $D_r=55\%$. It has been found that the results of BCR predicated on a large scale were greater than that of the model test by 13% and by about 18% for theoretical analysis. So, the validity of the test results is probable and these results may be applied for a large-scale foundation with consideration of the last-mentioned difference in the results.

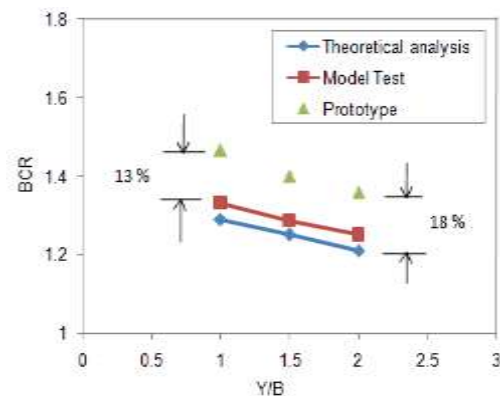


Fig. 14: Variations of BCR for a model test, theoretical analysis, and prototype with different depths of the soft pocket (Y/B) at $D_r=55\%$.

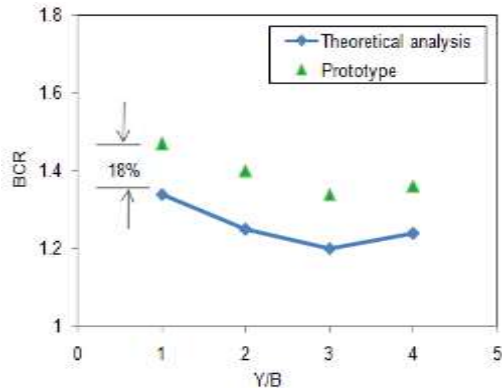


Fig. 15: Variations of BCR for theoretical analysis and prototype with different depths of the soft pocket (Y/B) at b/B=1.0, N=1, and $D_r=55\%$.

9. DEFORMATION CHARACTERISTICS AND FAILURE MECHANISM

In this section, the failure mechanism of strip footing on a reinforced and un-reinforced sand slope above an S. P. is investigated and discussed using the numerical output of the PLAXIS 3D Program.

For the case of footing above an S.P. and adjacent to a slope without geogrid, it can be seen that the failure model could be categorized as a perfect plastic failure with a circular slip surface as confirmed by Figs. 16 (a,b,c,d).

Despite existence of geogrid layers, the failure is modified to partial shear failure or punching shear failure with lesser deformation, which is noted from Figs. 16 (a,b,c,d). The existence of such reinforcement shows gradual improvement and control of the vertical and horizontal deformation [3,4,7,20].

Figs. 16 show the failure modes without reinforcement geogrid layers for different cases at Y/B=1.0, 2.0, 3.0, and 4.0 at b/B= 1.0 for $D_r=55\%$ at maximum stress for each one of them (for small-scale tank test). However, Figs. 17 shows the failure modes with reinforcement geogrid layers for different cases at Y/B=1.0, 2.0, 3.0, and 4.0 at b/B= 1.0 and N=1 for $D_r=55\%$ at maximum stress for each one of them (for small-scale tank test).

This again confirmed the effectiveness of using reinforcement to control the form of displacement and modify the failure pattern.

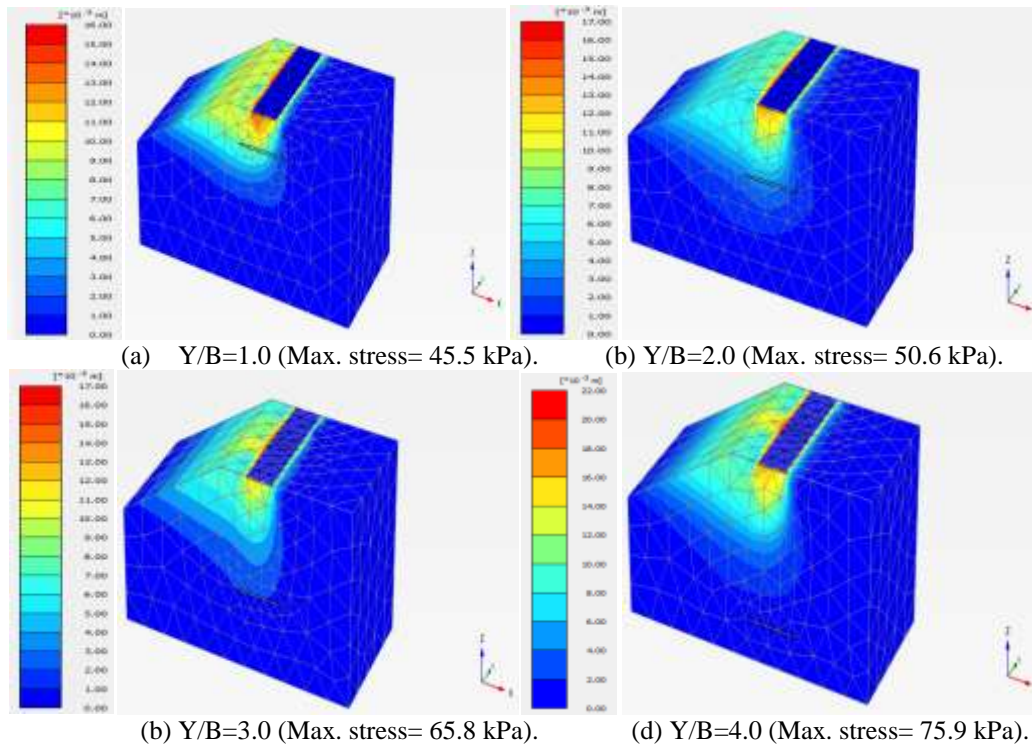


Fig. 16: Output PLAXIS 3D of total displacements for un-reinforced sand slope at b/B= 1.0 for $D_r=55\%$ for different depths of the soft pocket at maximum stress for each one of them (for small-scale tank test).

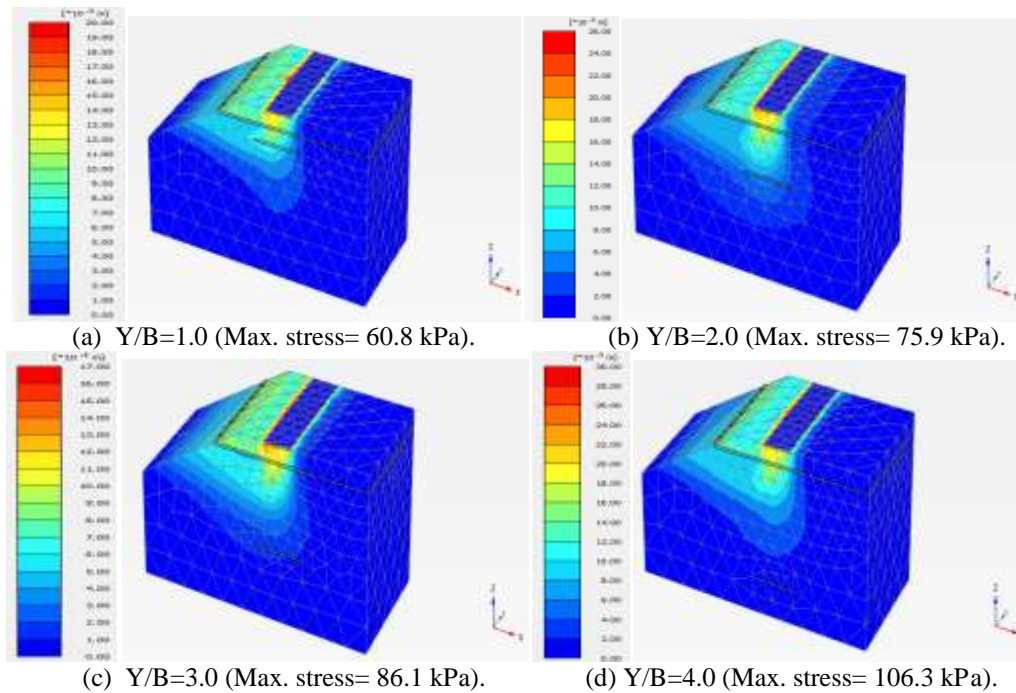


Fig. 17: Output PLAXIS 3D of total displacements for reinforced sand slope at $b/B=1.0$ and $N=1$ for $D_r=55\%$ for different depths of the soft pocket at maximum stress for each one of them (for small-scale tank test).

10. CONCLUSIONS

The main purpose of such a numerical analysis is to study the behavior of a strip footing adjacent to a reinforced slope above a soft pocket, taking multiple variables and factors into account, including the soft pocket depth, the setback distance from the crest of the slope to the strip footing, the number of reinforcement layers and the relative densities. The performed analyses indicated the following :

1. An existing soft pocket causes the ultimate bearing capacity (ultimate B. C.) to decrease, while its existence also increases the settlement of the footing. There is a critical region below the footing and the behavior of the footing is significantly affected by the presence of the soft pocket only when the Soft Pocket is located within this region. The ultimate B. C. of footing on sand slope 2(V): 3(H) decreased by 35% and 26% at $Y/B=1.0$ compared to the same case without a Soft Pocket at $b/B=1.0$ for $D_r=55$ and 80%, respectively.
2. The usage of soil reinforcement leads to a predominant improvement in the behavior of loaded footing on sand slopes above soft pockets as a result of reducing footing settlement and thus improving the overall behavior. The ultimate B. C. and the settlement at the ultimate B. C. of a footing near to reinforced sand slope above a soft pocket increased about 75% and 20%, respectively in

the case of $b/B=1.0$, $Y/B=1.5$, and $N=2.0$ compared to the same case without geogrid layers at $D_r=55\%$.

3. The inclusion of soil reinforcement results in additional remarkable improvements in the BCR of the footing, which increase with increasing the number of geogrid layers. When $N=1$ the BCR is 1.33 and when using $N=3$ it becomes 1.88 at $D_r=55\%$. However, this increase decreased to 1.154 and 1.69 at $N=1$ and 3, respectively at $D_r=80\%$.
4. The influence of a soft pocket on the BCR of sand is inversely proportional to the relative density of sand where the BCR increased by 22% and 20% at $D_r=55$ and 80%, respectively when Y/B decreased from 3.0 to 1.0 at $b/B=1.0$ and $N=1.0$.
5. The more the depth of the soft pocket below the footing is increased, the more the ultimate B. C. of the footing increases. Thereby, improvement is found to be decreasing. Therefore, it is concluded that the BCR is inversely proportional to the depth of the soft pocket below the footing. The BCR decreased by 27% and 19% at $D_r=55$ and 80%, respectively when the depth of the soft pocket increased from 1.0 to 2.0 below the footing in case of $b/B=0.0$ and $N=1$.
6. The effect of the slope on the footing behavior approximately decreased at the setback distance was equal to twice the footing width, especially at the dense sand state ($D_r=80\%$). The BCR values decreased by 37% and 28% when b/B increased from 0.0 to 2.0 at

Y/B=1.5 and N=2.0 for $D_r=55$ and 80%, respectively.

11. REFERENCES

- [1] Salih K.M. and Mustafa L., Model Studies of Bearing Capacity of Strip Footing on Sand Slope, *KSCE Journal of Civil Engineering*, 2012, 17(4), pp.699-711. <https://doi.org/10.1007/s12205-013-0406-x>.
- [2] Arash A.L., Ali T., Mahmoud G., and Tom S., Behavior of Shallow Strip Footing on Twin Voids, *Geotechnical, and Geological Engineering*, 2016, pp.1-18. DOI 10.1007/s10706-016-9989-6.
- [3] Haizuo Z., Gang Z., Xiaopei H., Xiaomin X., Tianqi Z., and Xinyu Y., Bearing capacity of strip footings on $c-\phi$ soils with square voids, *Acta Geotechnica*, Springer-Verlag GmbH Germany, 2018, pp.747-755, <https://doi.org/10.1007/s11440-018-0630-0>.
- [4] Yao X., Minghua Z., Heng Z., Heng Z. and Rui Z., Finite Element Limit Analysis of the Bearing Capacity of Strip Footing on a Rock Mass with Voids, *Int. J. Geomech.*, 2018, 18(9): 04018108, pp.1-15. DOI: 10.1061/(ASCE)GM.1943-5622.0001262.
- [5] Makoto K., Osamu K., and Masatoshi O., Model Tests and Analyses of Bearing Capacity of Strip Footing on Stiff Ground with Voids, *J. Geotech. Geoenviron. Eng.*, 2011, 137: pp. 363-375.
- [6] Mohamed M.H., Stability of strip footing on sand bed with a circular void, *Journal of Engineering Sciences*, Assiut University, Faculty of Engineering, 2014, Vol. 42, No. 1, January, pp. 1-17.
- [7] Salih K.M. and Mustafa L., Experimental and Numerical Studies of Strip Footings on Geogrid-Reinforced Sand Slope. *Arab J SciEng* (2014) 39, pp.1607-1619. DOI 10.1007/s13369-013-0795-7.
- [8] Mostafa A. El-S. and Ashraf K.N., Cyclic settlement behavior of strip footings resting on a reinforced layered sand slope, *Journal of Advanced Research* (2012) 3, pp. 315-324. Doi:10.1016/j.jare.2011.10.002.
- [9] Mostafa A. El-S., Waseim R.A., and Engy M.K. Bearing capacity of a strip footing adjacent to a sand slope with soft pocket, *International Conference on Advances in Structural and Geotechnical Engineering 2021*, pp.29-31 March, Hurghada-Egypt.
- [10] Mostafa A. El-S., Waseim R.A., and Engy M.K., An Experimental Study of the Behavior of a Strip Footing Adjacent to Reinforced Sand Slope Above a Soft Pocket, *International Journal of GEOMATE*, Nov. 2021, Vol. 21, Issue 87, pp.118-127. DOI: <https://doi.org/10.21660/2021.87.j2369>.
- [11] Ashraf N. and Ahmed N., Pullout capacity of batter pile in the sand, *Journal of Advanced Research*, 4(2013), pp.147-154.
- [12] Dharmatti, V. and Rakaraddi, G., An experimental study on vertically loaded driven and cast-in-situ piles, *Journal of Mechanical and Civil Engineering (JMCE)*, 2014, 11(2), pp. 43-48.
- [13] Mohamed A.S., Ashraf K.N., Waseim R.A., and Ahmed F.S., Model study of a single pile with wings under uplift loads, *Journal of Applied Ocean Research*, 100 (2020), pp.102-187. <https://doi.org/10.1016/j.apor.2020.102187>.
- [14] Calogero V., Maurizio Z., and Sandro R. M., The bearing capacity of footings on the sand with a weak layer, *Geotechnical Research*, 2017, Volume 4 Issue GR1, pp. 12-29. <http://dx.doi.org/10.1680/jgere.16.00020>.
- [15] Anil K. S.V. and Ilamparuthi K., Response of footing on sand slopes, *IGC 2009*, Guntur, INDIA, pp. 622-626.
- [16] El Rahman A.A., Nagy N.M., Kamal I.M. and Hassan, M.A., Finite element analysis of reinforced sand under the circular footing, *IOP Conference Series*, 2020, 974(1), 012004, pp.1-13.
- [17] Belal A., Nagy N. and Elshesheny A., Numerical evaluation of bearing capacity of square footing on geosynthetic reinforced sand, *Proceedings of the 2nd International Conference on Civil, Structural and Transportation, Engineering*, Canada, May 2016, pp. 1-9.
- [18] Tapan K.N., Koushik H. and Debarghya C., Experimental Investigation on the Behaviour of Geogrid-Reinforced Soil Slope under Strip Loading, *Indian Geotechnical Conference 2017*, IIT Guwahati, India, pp. 1-4.
- [19] Rana A. and Arindam D., Bearing Capacity of Strip Footing Resting on the Crest of a Slope: FE Simulation, *Indian Geotechnical Conference 2017 GeoNest*, 14-16 December 2017, IIT Guwahati, India, pp.1-4.
- [20] Yao X., Minghua Z., and Heng Z., Undrained stability of strip footing above voids in two-layered clays by finite element limit analysis. *Computers and Geotechnics* 97 (2018), pp.124-133. DOI: [10.1016/j.compgeo.2018.01.005](https://doi.org/10.1016/j.compgeo.2018.01.005).